



Controlling microstructural and mechanical properties of direct laser deposited Inconel 718 via laser power



Abdullah Alhuzaim^{a,b}, Stano Imbrogno^a, Moataz M. Attallah^{a,*}

^a School of Metallurgy and Material Sciences, University of Birmingham, Edgbaston, Birmingham B15 2TT, United Kingdom

^b Mechanical Engineering Department, Jubail University College, Jubail Industrial City, Kingdom of Saudi Arabia

ARTICLE INFO

Article history:

Received 18 November 2020

Received in revised form 9 February 2021

Accepted 17 March 2021

Available online 22 March 2021

Keywords:

Ni-superalloys

Direct laser deposition

Microstructure

Segregation

ABSTRACT

The control of grain structure, texture and micro-segregation during additive manufacturing is important due to their impact on the mechanical properties. In this work, multiple single walls were deposited using Inconel 718 powder by the Direct Laser Deposition (DLD) process. The influence of a wide range of laser power (150–1900 W), as well as the thermal gradient, were characterized using electron microscopy and hardness testing. The heat input effect on the microstructural, dendritic morphology, and microhardness was also examined. The results illustrated that a higher thermal gradient due to lower heat input tends to form equiaxed grains and more Nb-segregation, whilst a higher heat input develops columnar grains with low Nb-segregation. The segregations within the interdendritic boundaries increased in size when the heat input was increased, whilst the contribution from precipitation strengthening was not significantly evident in the as-fabricated condition. A wall with two different powers was also deposited to demonstrate the possibility of creating functionally graded structures through the control of laser power.

© 2021 Elsevier B.V. All rights reserved.

1. Introduction

DLD is a technique where components are built layer-by-layer by blowing powder through a nozzle and melting with a focused laser beam. It has been used extensively within the aerospace and energy sectors, particularly in repairing turbine and steam engine blades. DLD is also recognized as a process with the ability to produce complex geometric components and with the flexibility to repair damaged or worn parts, with less powder consumption compared to laser powder bed fusion [1,2]. It is considered one of the most rapid near net-shape techniques because of its large spot size, layer thickness and deposition rate. It is known that as-fabricated builds typically have poor mechanical properties compared to the post-deposition heat-treated parts. The focus of this study is to develop as-fabricated structures with reasonable properties, as a quick introduction to the market and the speed of delivering the part can be crucial in some fields.

Turbine blades can be manufactured in multiple ways. The traditional method is conventional casting which usually produces equiaxed crystal structures, providing isotropic mechanical properties, higher tensile strength and fatigue resistance. An alternative

production technique is directional solidification which allows the production of large directionally solidified grains in the blade leading to good creep deformation resistance, improved oxidation resistance and enhanced mechanical properties along the solidification direction. In contrast, the fir tree root of the blade requires high tensile strength due to centrifugal loading and high/low cycle fatigue resistance, therefore the microstructure has to show different characteristics compared with the blade body [3]. The scope of this study is on single-wall deposition due to its potential from a repair perspective, especially in the repair of turbine blade tips and seal segments. The study focused on the laser power impact on the microstructural development, due to the ease of modifying the laser power on the fly (as a single parameter), compared with changing the other parameters (e.g. powder flow rate, laser speed, etc...). Of a greater interest, the study assesses the possibility of matching the grain structure of the substrate or component being repaired through controlling a single parameter.

The Ni-based superalloy Inconel 718 (IN718) is widely used in aerospace applications due to its good formability, high corrosion resistance and excellent mechanical properties up to 650 °C [4]. During DLD of IN718, rapid heating, melting, solidification and rapid cooling processes are involved, and these affect the liquid-solid interface during solidification through fast diffusion of the Nb [2]. The different thermal gradients and the growth rate control the

* Corresponding author.

E-mail address: m.m.attallah@bham.ac.uk (M.M. Attallah).

morphology and solidification of the grains structure whilst the direction of the growth of the grains usually follows the heat source.

During the deposition process, the heat source is perpendicular to the molten pool towards the previous layer or the substrate since the lower ratio of the thermal gradient (G) and solidification rate (R) near the top surface of the molten pool results in equiaxed grains. Hence, columnar dendrites are observed to grow from the substrate perpendicular to the edge of the welding pool. The solidification velocity and the temperature gradient are responsible for forming columnar or a mixture of columnar and equiaxed dendrites towards the heat source direction [3,4].

During solidification, several Nb atoms are constantly rejected and segregated into the liquid around the dendrites while the solid γ phase is forming from the liquid phase. After the γ phase formation, the low solubility of Nb results in its continuous ejection and accumulation at the liquid phase. As the solidification proceeds, the chemical composition of the liquid phase will shift towards the eutectic point. Lastly, the liquid phase transforms into the γ phase and the segregated Nb from the interdendritic phase reaches the eutectic point by a eutectic reaction [5].

During DLD, the solidification process is comparable with the one observed during welding. Therefore, the expected microstructure is dendritic and characterized by micro-segregation due to the thermal cycle and high cooling rate. Chen et al. [6] used DLD to produce single-track thin walls and they claimed that the Laves phase had the highest fraction in the middle of the sample due to high accumulation of heat and a low cooling rate. It had the lowest fraction at the bottom and the top of the sample due to a high cooling rate and less accumulated heat. Therefore, it is clear that the cooling rate can govern the segregation rate during solidification. Furthermore, they also claimed that there is an inverse correlation between the Nb concentration of the Laves phase and the cooling rate since the element diffusion would have insufficient time when the cooling rate increases [7]. However, the effect of different laser powers on the microstructure and mechanical properties was overlooked since they focused their study on liquation crack formation.

Parimi et al. [8] found that DLD high laser power generates columnar grains structures with $\langle 001 \rangle$ fiber texture along with the build directions and a mixture of fine equiaxed and coarser columnar grains in the low power samples. It was demonstrated that DLD is capable of tailoring the grain structure depending on the process parameters and the deposition strategy. Zhu et al. [9] also studied the influence of various parameters on the as-deposited Inconel 718 at different laser power and laser beam diameter. The columnar grains enlarged with increasing laser power and laser beam diameter. Ding et al. confirmed that the dendrite core microstructure can be linked to the cooling rate [10]. A high cooling rate showed a fine dendrite core, nearly continuous inter-dendritic regions, whilst a low cooling rate led to coarse dendritic regions and semi-continuous interdendritic regions. On the structural integrity front, Zhong et al. [11] showed that porosity can be reduced by increasing the laser power [12].

The solidification regimes remain the key factor in controlling the microstructure. Raghavan et al. [13] showed that control of the crystallographic texture of the components can be achieved, to some extent, by governing the variations of (G) temperature gradient and (R) growth velocity at the liquid-solid interface of the melt pool. The results of the model indicated that by increasing the height of the wall, the rate of the heat removed by conduction by the substrate was decreased, thus leading to higher heat accumulation. This led to an increase in the grain size due to the increase in the height of the wall [14].

There are numerous current studies on DLD of IN718, but they appear to demonstrate the following gaps. Firstly, the majority of the studies focus on two extremes such as low and high power, with no experimental evidence on the microstructural variations between

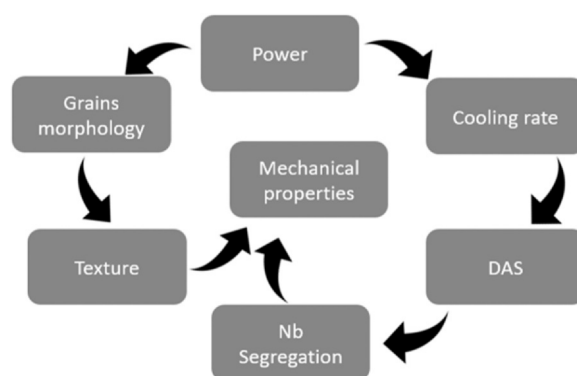


Fig. 1. Schematic diagrams showing the effect of power on the microstructure and mechanical properties.

the upper and lower laser power limits. None of the studies explain the effect of the layer thicknesses on grain size and morphology. Moreover, limited studies explored the possibility of using different laser powers during DLD to explore the possibility of creating a functionally graded microstructure. In this study, the development in grains size, their morphology and texture was investigated in IN718 single wall builds. The effect of different laser powers on the microstructural characteristics and Nb segregation and, therefore, mechanical properties were analysed in detail.

The aim of this investigation is to demonstrate the utility of DLD parameters in tailoring the as-fabricated IN718 microstructure through controlling the solidification pathways. The solidified microstructure as demonstrated using the dendrite arm spacing (DAS) can be correlated with the solidification mechanisms and cooling rates. Finally, a strategy for parameter control and prediction of the microstructure and the mechanical properties of the fabricated IN718 superalloy by changing the laser power in the DLD process also developed and discussed (Fig. 1).

2. Experimental procedures

Thin walls were produced using the Trumpf TLC 1005 system equipped with a three-beam nozzle able to move on a cartesian space (x , y and z) and a 4 kW diode laser (Trumpf TrueDisk 4002) system. Gas atomized IN718 powder (supplied by Carpenter Additive) with limited satellite formation was used, as shown in Fig. 2. The powder was sieved in the range from 53 to 180 μm , as required by the DLD process due to its ease of flow through the nozzle. The chemical composition was analysed by AMG Superalloys UK Limited using Inductively Coupled Plasma (ICP). The chemical composition is shown in Table 1.

During deposition, the laser beam focused on a spot size of 1.4 mm while the standoff distance between the laser head and the surface of the substrate was set to 10 mm. The laser operative regime was set as continuous wave (CW). A three-beam nozzle was used, providing a constant powder flow rate of 25 g/min and positioned with a 10 mm distance from the substrate, in order to achieve a defocusing distance for the powder stream of 2 mm (D_p in Fig. 3). The focus of the laser beam was set in order to attain a positive defocusing of 3 mm above the surface of the substrate (suggested by D_L in Fig. 3) This configuration allowed the triggering of the auto compensation of the deposition during the process in order to avoid uneven horizontal surfaces of the walls. Fig. 4 shows the setup of the experiment. Four K-type thermocouples were inserted into holes located 1 mm below the substrate surface. Two infrared cameras (acquisition filter from 150 $^{\circ}\text{C}$ to 2000 $^{\circ}\text{C}$) were used to identify the thermal gradient during deposition.

The scanning speed parameter was kept fixed to 11.7 mm/s. whilst the scan strategy was set as bidirectional with a layer

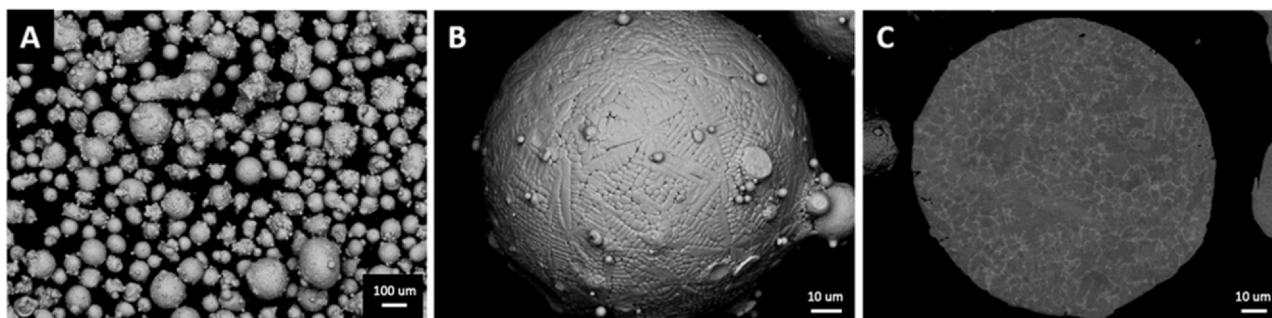


Fig. 2. A) SEM of the gas atomized IN718 Powder Particles, B) micrograph showing the surface of a large particle, C) dendrite morphology inside powder particle.

thickness of 0.5 mm as shown in Fig. 5. Each wall was built by depositing 40 layers with a length of 30 mm along the x-direction. The thin walls were produced at a very low oxygen level due to the argon delivered by the laser head in the carrier gas that was flowing from the nozzle. The argon also protected the lens from rebounding particles from the build. The IN718 substrates were machined to an upside-down T shape.

Table 2 reports the process parameters used and the energy density E (J/mm^3) calculated using Eq. (1) where LP (W) is the power of the laser and VI refers to the scan speed (mm/s), L_d is the laser spot size (mm).

$$Es = Lp/(LdVI) \quad (1)$$

However, due to the wide range of laser powers that were investigated which will affect the spot size diameter, a simpler equation (Eq. (2)) was used, where P is the laser power (Watt) and V is the scanning speed (mm/s) [15].

$$\text{Heat input (HI)} = P/V \quad (2)$$

As shown in Table 2, the different laser power levels were investigated while the scan speed and the powder feed were kept constant in order to study the effect of only the laser power.

2.1. Characterisation methods

After DLD, the thin wall builds were cut using wire electric-discharge machining (EDM) into 3 mm samples in the XY dimension, then they were hot mounted in Bakelite, ground and polished to $0.04 \mu\text{m}$ colloidal silica suspension finish. Subsequently, the samples were electrolytically etched using 10% phosphoric acid (H_3PO_4) and 90% H_2O for 30 s using a voltage of 5 V. This procedure permitted the revealing of the microstructure that was investigated using a Hitachi 3000 Scanning Electron Microscope (SEM) equipped with a back-scattered electron (BSE) detector. The pictures acquired were analysed using ImageJ. A Philips XL-30 SEM equipped with an electron backscatter diffraction detector (EBSD) and operated at 20 kV with a spot size of 6 nm was used to reveal the crystallographic texture due to DLD. The EBSD maps were imaged at $120\times$ magnification and a $3.0 \mu\text{m}$ step size.

Grain size analysis was carried out using the linear intercept method. X-ray diffraction (XRD) was performed using a Bruker D2 Cobalt diffractometer, Co- $\text{K}\alpha$ radiation ($\lambda = 1.79 \text{ \AA}$) with a step of $0.02^\circ 2\theta$, a scan speed of 11.7 s/step and 2θ angle ranging from 40° to 120° . Micro-hardness ($\text{HV}_{0.5}$) was measured using a micro Vickers MMT-X from MATSUZAWA.

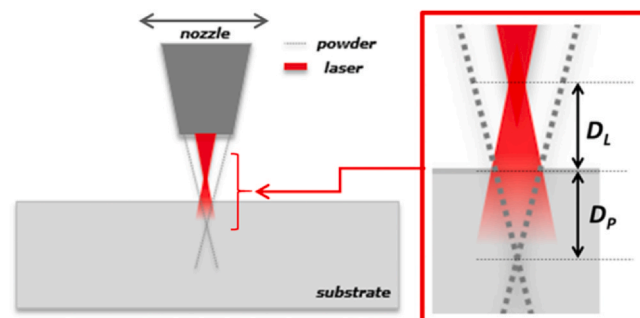


Fig. 3. Schematic illustration of the powder stream defocusing (D_p) and laser beam defocusing (D_l) distance.

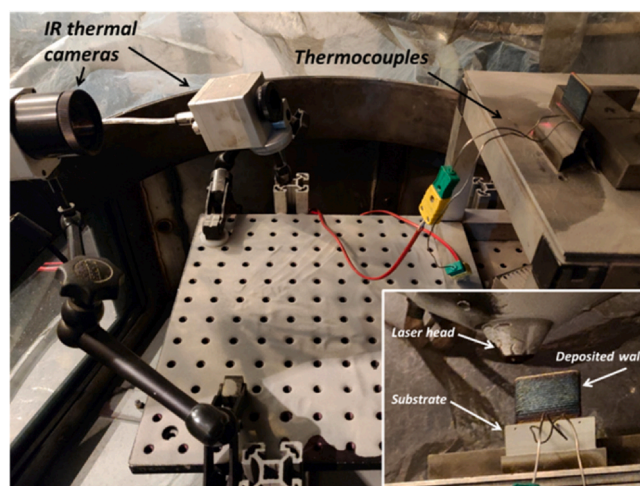


Fig. 4. Experiment set up using the Trumpf, thermo-cameras and thermocouples.

3. Results and discussion

The depth of penetration (DP) and weld pool width (WPW) are normally influenced by the different process variables in DLD. However, in this study, the laser scanning speed, laser spot size, stand off distance and powder feed were fixed. Still, the results showed that both the WPW and DP increase with the increase in laser power, from ~ 0.25 to 1 mm range at 150 W reaching $1.5\text{--}3 \text{ mm}$ range at 1.9 kW . Both quantities are useful in assessing the degree of

Table 1
Powder chemical analysis for IN718 (wt%).

Ni	Cr	Fe	Nb	Mo	Ti	Al	Si	Ta	C	S	N	O
54.45	18.18	18.19	4.88	2.9	0.91	0.42	0.03	0.02	0.01	0.002	0.01	0.011

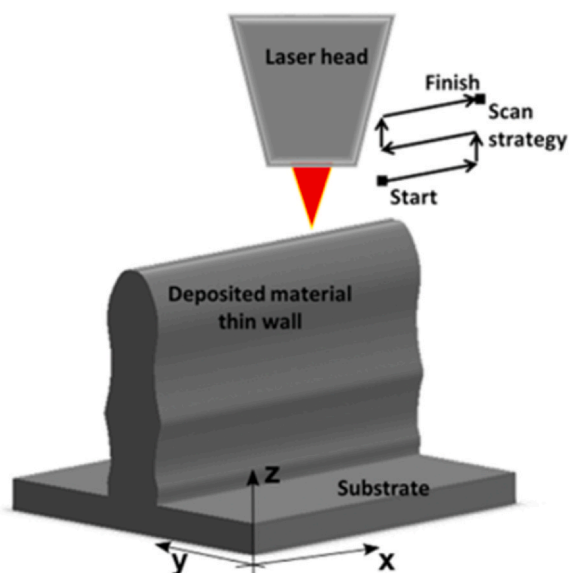


Fig. 5. Schematisation illustration of the laser metal deposition process depositing material of the thin wall and the scan strategy.

Table 2
Process parameters of single walls.

Sample	Power (W)	Scanning speed (mm/s)	Powder feed (g/min)	Heat input (J/mm)
CW 150	150	11.7	25	12.8
CW 200	200			17.1
CW 300	300			25.6
CW 400	400			34.2
CW 500	500			42.7
CW 700	700			59.8
CW 900	900			76.9
CW 1100	1100			94.0
CW 1300	1300			111.1
CW 1500	1500			128.2
CW 1700	1700			145.3
CW 1900	1900			162.4

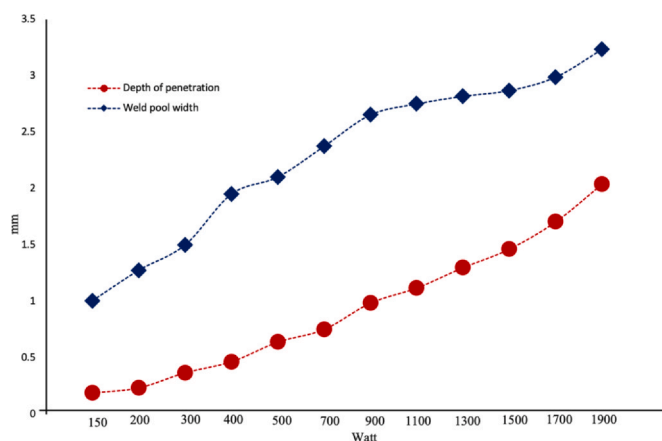


Fig. 6. Depth of penetration and weld pool width.

attachment between the newly added layers and the substrate or the prior layers (Fig. 6).

3.1. The effects of laser power on microstructure morphology

The columnar-to-equiaxed grains transformation is caused by low solidification velocity and low thermal gradient, while the

directionality of the microstructure is a specific characteristic particularly observed when metallic materials are processed using DLD. Columnar-to-equiaxed transition usually occurs when the actual temperature is lower than the equilibrium liquid temperature [16]. During the deposition of the first layer of material on the substrate, the columnar grains start to form, and they grow epitaxially following the direction of the heat source, the laser beam. Subsequently, more layers are deposited, and more columnar grains continue to nucleate and grow epitaxially from the grains formed in the previous layers. Consequently, the elongated epitaxial columnar grains grow continuously through multiple layers [17].

The EBSD maps show the inverse pole figure maps of samples extracted within the middle region of each wall, approximately 10 mm from the bottom of the sample, Fig. 7. It is worth highlighting that low laser power (LP) leads to the formation of a microstructure that is characterized by a mixed structure of equiaxed grains and elongated grains along the build direction. High laser power (HP), however, leads to a structure with coarse elongated grains that extend columnarly along the build direction which mainly grow following the heat flow path. This is because, when the laser power increases, the weld pool expands which results in a lower thermal gradient and a slower cooling rate compared to the samples with lower power [18]. It can also be observed that the presence of a finer grain structure with random crystallographic orientations leads to a weaker texture intensity in the low power conditions. As concerns the texture, Fig. 7 illustrates that low laser power produces parts with a weak cubic texture while high laser power produces a spotty.

The grains size distribution (estimated using the equivalent diameter of the grain area) was measured from the EBSD results and is shown in Fig. 8. Equiaxed and columnar grains with different diameters were observed. When using low laser power (150 W), no columnar grains were observed, only fine equiaxed grains were observed with an average diameter of 15 μm . When the laser power was increased to 500 W, columnar grains of different lengths/widths nucleated and grew to an average grain size of 40 μm , with the grains extend to ~100 μm in length along the build direction and ~50 μm in width. The highest laser power used in this investigation showed large columnar grains with an average grain size of 70 μm .

The grain structure of the high laser power samples was characterized by elongated columnar grains that extended across multiple layers. Conversely, the texture observed in the samples produced by low laser power, a mixture of equiaxed and columnar grains with a significant amount of small equiaxed grains in the upper part of the layers and on the side of the build was observed. This was mainly due to the enhanced high cooling rate that affected the solidification rate and thermal gradient, that is compatible with the explanation proposed by Wei et al. [17]. Moreover, Wei et al. [19] found that epitaxial columnar grain growth occurred from the previously deposited layer or the substrate to the curved top surface and continued to grow because of the cyclic heating and cooling during DLD. The columnar grain area increases by approximately 80% when moving from the edge to the center of the deposit. This is because of the variable growth directions dependent on the moving molten pool. Due to repeated thermal cycling and remelting, a gradual increase in grain size is noted between the successive layers, with a 20% increase in grain width from the third to the eighth layers.

3.2. The effect of laser power on grain size and growth orientation

Because DLD technology is used to perform repair or coating of already existing metal parts, the control of the crystallographic texture is extremely important. As suggested by the results of this study, some geometrical aspects of the microstructure can be controlled to some extent by manipulating the laser power. Therefore, in order to match the grains of the repaired part to its parent material, understanding the transformation from equiaxed to columnar grain

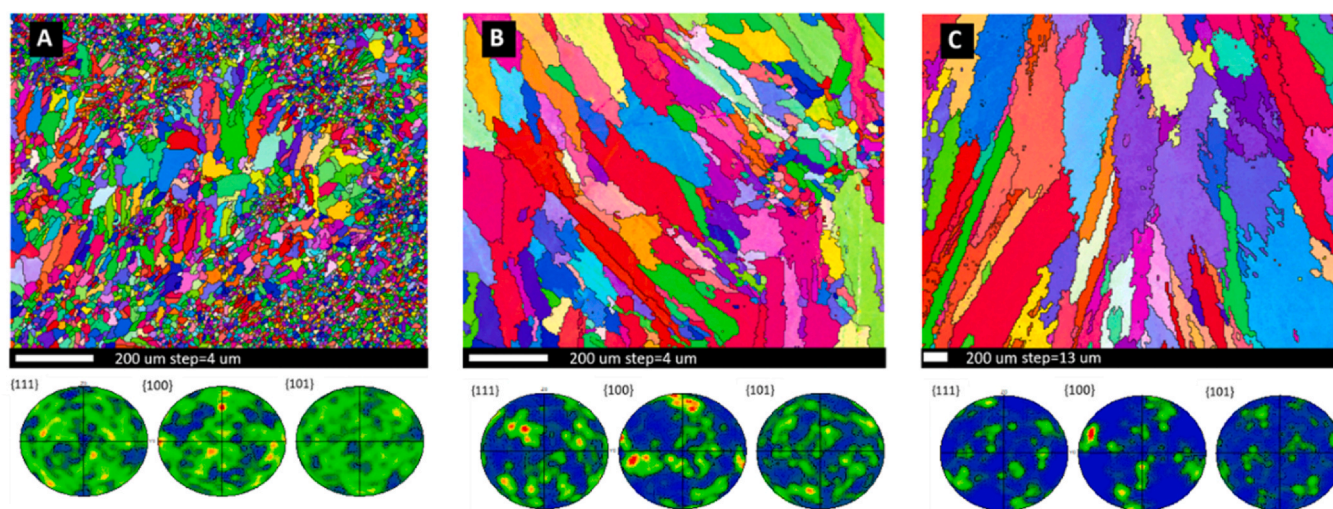


Fig. 7. EBSD map of IN718 samples produced by a continuous wave in the building direction with no PWHT (A) 150 W (B) 500 W (C) 1900 W. The build direction is the vertical axis of the map.

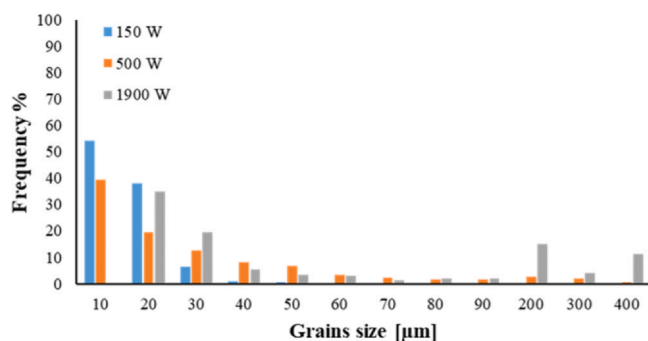


Fig. 8. Frequency percentage of grain size produced by three different laser powers.

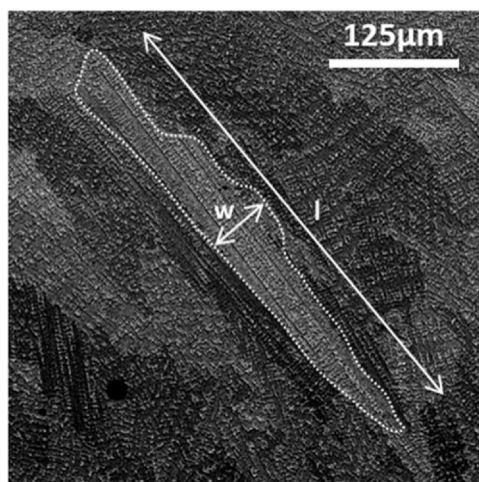


Fig. 9. Length and width of a columnar grain.

due to the level of laser power must be considered. Generally, a columnar microstructure is dominant in DLD. Generally, the columnar grain is quantified by two geometrical features that are length (l) and width (w) of the grains (Fig. 9). Fig. 10 illustrates the grains map that provides an estimation of the length and width of the grains depending on the laser power.

As shown in Fig. 10, laser power between 150 W and 200 W gave an aspect ratio close to one, which suggests that the grain structure

is approximately equiaxed. The increase of power in the range of 300–500 W affected the grain morphology, whereby the structure started to become columnar (increasing in length) but still maintaining a similar width of the grains produced with lower laser power. In the range of 500–700 W, the grains continued to grow longitudinally, but the width started to increase too. In the range of 700–900 W, the width reached a steady state whilst a slight increase in the length of the grains was still evident. Finally, in the range of 900–1900 W, the width was still constant, and the length reached a steady state. In particular, it was observed that after every 200 W the width increased significantly until it reached a constant value.

Columnar grains provide maximum high-temperature mechanical performance along the loading direction. However, for applications with multidirectional stress applied to the component, the anisotropy is detrimental [12]. Therefore, microstructure control during the deposition process plays an important role. As showed in Fig. 10, lower laser powers permitted the achievement of a very low heat accumulation in the deposited material, thus enhancing the cooling rate. Experimental evidence of the different levels of accumulated heat using thermal imaging is shown in Fig. 11. It is possible to observe that increasing laser power will increase the accumulation of heat in the wall and particularly, from the central region up to the top of the wall, it is significantly higher. This result confirms the substrate's impact on reducing the temperature within the first layers deposited, acting as a heat sink. According to Raghavan et al. [13], this resulted in having more equiaxed than columnar grains in the microstructure.

Another microstructural detail is represented by the demarcation, that is, the banded structure caused by rapid cooling. In the produced samples, different angles of demarcation were observed depending on the laser power used. Therefore, the angles were measured as showed in Fig. 12. The angle was lower than 130° when very low power was used and increased to a constant value (180°) when the power was increased. When laser power higher than 400 W was used the demarcation disappeared. Demarcation enhances tensile strength and prevents crack propagation; thus, it is an important feature in DLD microstructures [20].

3.3. The effect of laser power on Nb-segregation

SEM analysis was performed on the cross-section of samples (X-Z plane). As shown in Fig. 13, the austenite matrix γ phase was the dark grey phase, and the interdendritic Laves phase and Nb-segregation were brighter in contrast (mass contrast). The Laves and Nb-rich phases formed a network around dendrite cells.

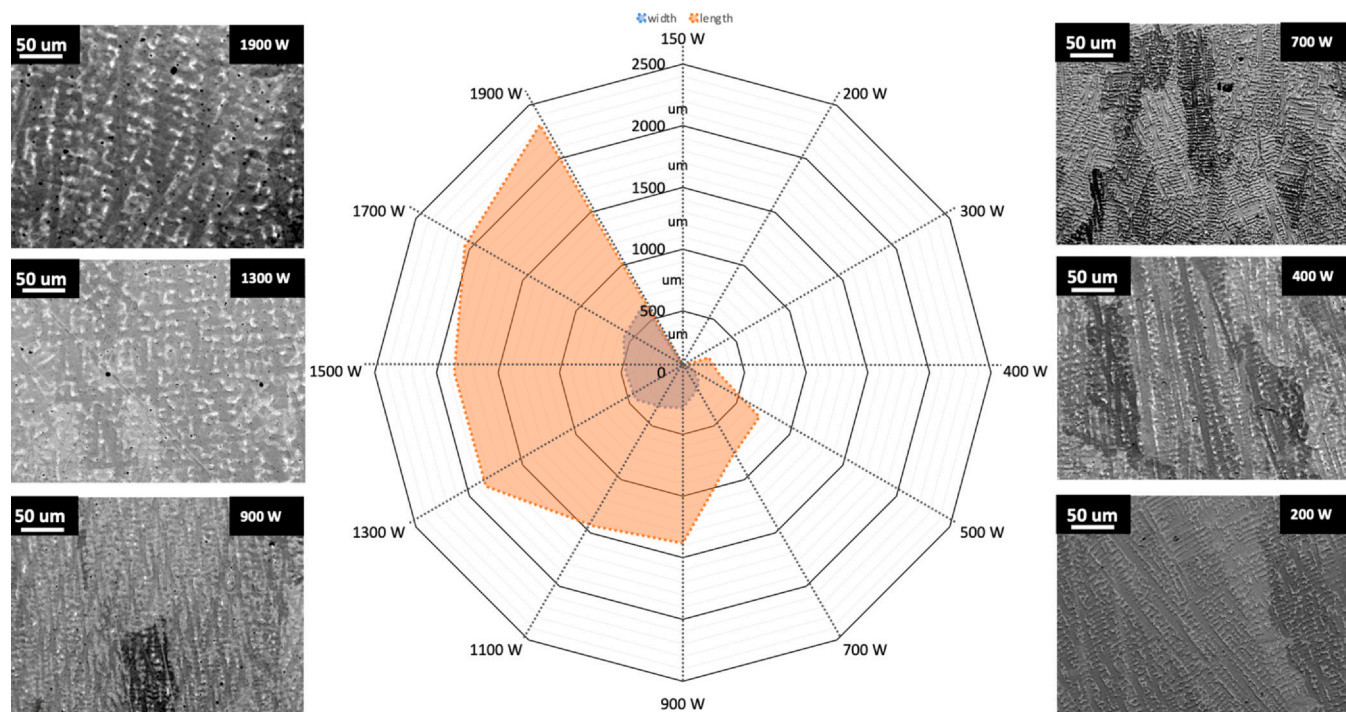


Fig. 10. Laser power effect on the morphology of the grains.

Nb-segregation is dependent on the cooling rate and the thermal history of the build. The bottom part of the thin wall showed the highest concentration of Laves phase, usually small and widely distributed. This area was connected to the substrate which acts as a heat sink. Therefore, in this area, a higher cooling rate was observed. The part of the sample in the middle of the build showed a decrease in the Laves phase fraction and a change in their morphology. This area usually experiences an accumulation of the heat cycles during the deposition of the layers. It is contrary to that observed by Chen et al. [7] where they claimed that the Laves phase fraction was highest in the middle of the sample due to the lower cooling rate and higher accumulation of heat, whilst the top and the bottom parts of the thin wall experienced higher cooling rate and therefore, lower Laves phase fraction. Moreover, it is important to highlight that in this study the overall Nb-segregation was quantified instead of only the Laves phase since the latter has a different chemistry (Nb, Mo, etc). The top part of the sample showed an increase in Nb-segregated region and percentage compared to the middle section. This area usually experiences very rapid cooling by convection and radiation because it is exposed at the top of the build.

3.4. The effect of laser power in Nb-segregation distribution and dendritic microstructure

The microstructure of as-deposited IN718 superalloy shows the different values of dendritic arm spacing (DAS) and Nb segregation with variation of power due to the influence of the cooling rate. The samples produced by low laser power (150–300 W) experienced a higher cooling rate and, therefore, a higher solidification rate, which produced fine equiaxed dendritic structures with fine and scattered Nb-segregation. The samples produced by higher laser power (400–1900 W) showed formation of long chain-like Nb-segregation. Fig. 14 shows the metallographic morphology of dendrites with the different power values.

Fig. 15 demonstrates variation in DAS and the Nb-segregation (quantified in area %) depending on the laser power used during the tests. The dendrite arm spacing is due to the increase in the heat input and a decrease in the solidification rate. When the heat input was increased from 12.86 J/mm (150 W) to 163 J/mm (1900 W), the average DAS increased from 7 μm to 20 μm. The Nb-accumulation on the area fraction reduced from 8% to 2%.

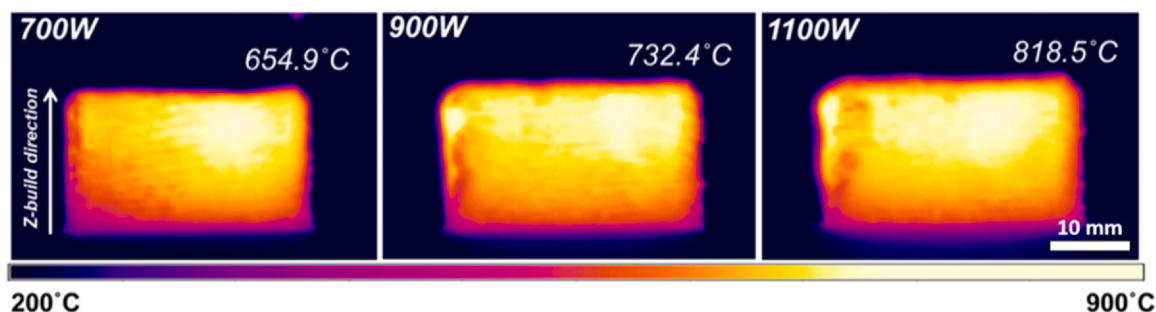


Fig. 11. Thermal imaging at three different power levels after exactly 1 min of shutting off heat source.

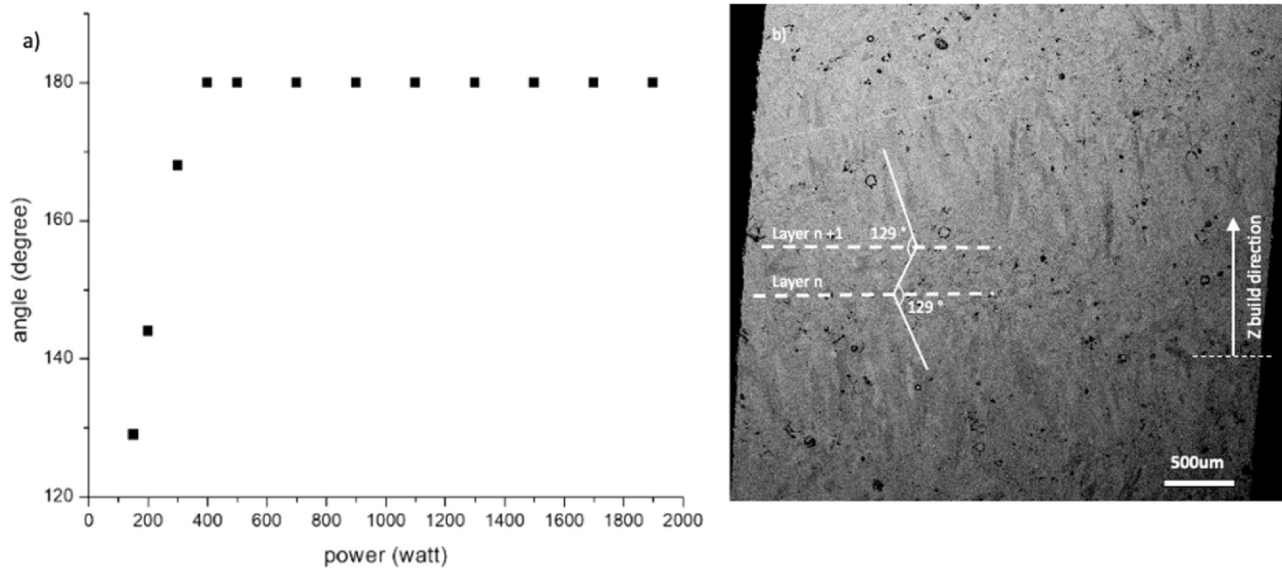


Fig. 12. Effect of laser power on the demarcation angle.

3.5. Correlating the microstructure and the cooling rate

As observed in the previous results, the heat accumulated is directly related to the laser power used. This is also responsible for the cooling rate of the material during the deposition process. It is also well known that the cooling rate has a direct effect on DAS, and this relation can be described mathematically by Eq. (3) [1].

$$\lambda = 80\varepsilon^{-0.33} \quad (3)$$

where λ is the primary dendrite arm spacing and ε is the cooling rate in K/s. Eq. (3) correlates the cooling rate and the DAS considering the calculated solidification rates in relation to the heat input studied in this work [7]. The amount of Nb segregation was higher in the low power samples because of the effect of the cooling rate associated with the heat input. This result was also observed by Zhu et al. [26].

As illustrated in Fig. 7, the grains transform from equiaxed to columnar with an increase of power which inversely affects the

thermal gradient and solidification velocity. In DLD the solidification is directed toward the thermal gradient (i.e. in the direction of the heat source) and the solid-liquid interface speed can be controlled by the heat input or by the travel speed. Depending on the power level, a columnar to equiaxed transition may occur and usually, this happens when the temperature is lower than the equilibrium liquid temperature [16].

Fig. 16 shows the cooling rate values obtained using DAS measurements and Eq. (2). Moreover, the relation between the DAS and the laser power is also plotted. This graph clearly demonstrates that when laser power is limited to low values (e. g. 150 W), very fine DAS can be expected (approximately 5 μm) and only a high cooling rate can form smaller microstructures characterized by small DAS.

Therefore, it is possible to observe that when the heat input increases, the DAS also increases while the cooling rate decreases. A decrease in the cooling rate usually is due to a decrease of the thermal gradient or a decrease in the velocity of the solidification front. Because

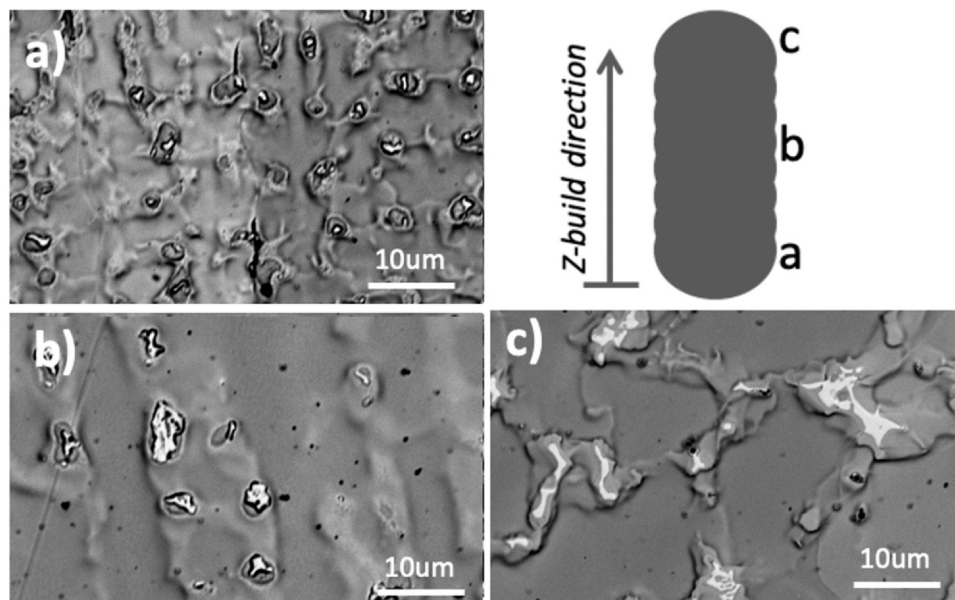


Fig. 13. Continuous waving single wall sample with laser power of 1100 W and scanning speed of 700 mm/min (A) Bottom (B) middle (C) top.

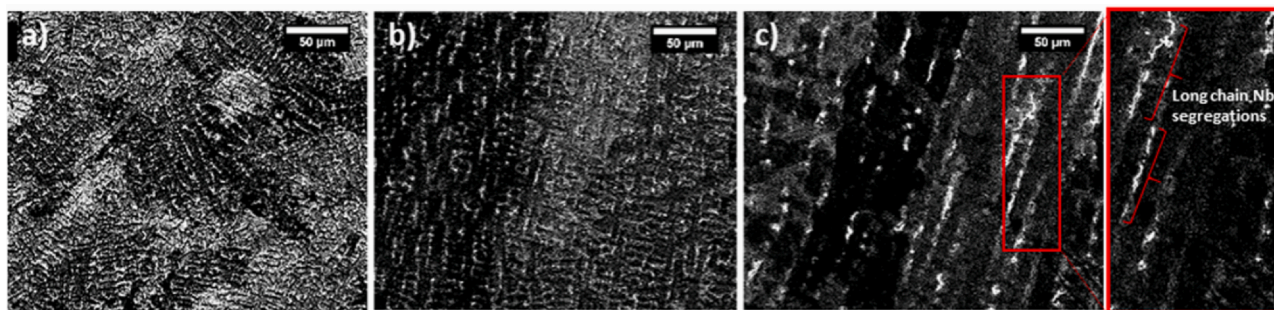


Fig. 14. SEM metallographic morphology of dendrites CW (A) 150 W (B) 900 W (C) 1900 W.

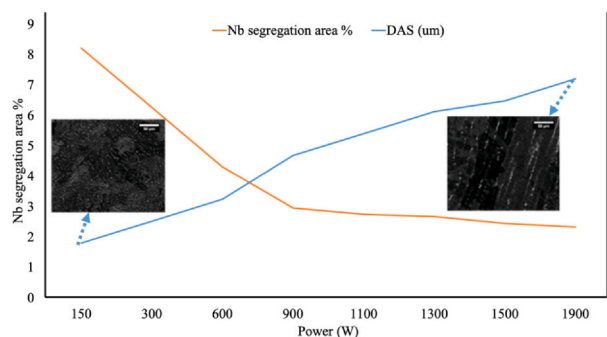


Fig. 15. Power effect on the percentage of Nb segregation and DAS.

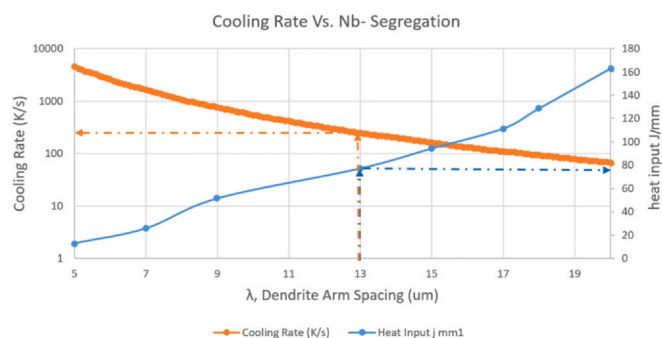


Fig. 16. The effect of cooling rate and power on dendrite arm spacing.

the scan speed is kept constant during all the tests, the variation of the cooling rate could be mainly related to the laser power.

3.6. The effect of laser power on hardness

The as-fabricated builds typically have poor mechanical properties compared to wrought products due to the presence of detrimental phases and the lack of strengthening phases. However, Qi et al. [21] showed that mechanical properties can be improved by performing a homogenization heat treatment at $\sim 1100^\circ\text{C}$ for 1–2 h, followed by a solution treatment and aging to allow the precipitation of the strengthening γ'' and γ' phases. Although the γ'' phase is the main strengthening phase in IN718, the rapid solidification that occurs during DLD does not enable its formation due to its sluggish nature. It is important to highlight that, in this study, only the as-fabricated condition was investigated due to the study focus on grains size control. Post heat treatment below the recrystallization temperature can be used to improve the mechanical properties without affecting the grains size and morphology.

The hardness results of the three specimens with different power levels are plotted in Fig. 17. The obtained results appear to suggest a possible relationship between hardness and grain size. A primary

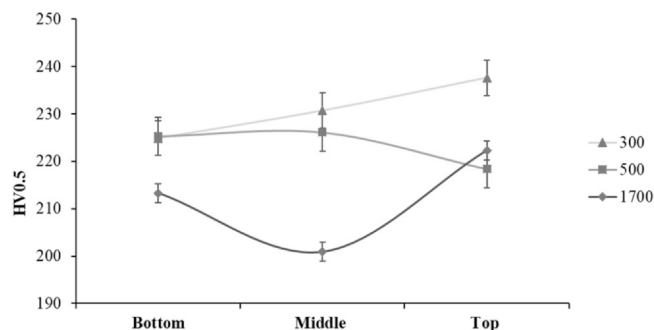


Fig. 17. The effect of laser power effect on hardness (cross section of the samples).

factor of increasing hardness in IN718 is the precipitation phenomena. In this case, a lower laser power such as 300 W led to gentle heating and accumulation of heat, provoking what seems to be limited aging which may promote the formation of strengthening phases (γ' and γ''), since γ' and γ'' phases precipitate between 600 and 900°C . Moreover, the γ' can form in a shorter time and requires less heat than the sluggish γ'' [22]. On the contrary, laser power of 1700 W led to an extremely high temperature and a significant accumulation of heat, therefore, the Nb tends to dissolve into the matrix.

The grain size might also affect hardness results. In general, the smaller the grain size is, the harder the material is and since lower power produces smaller grain size, the greater hardness could be justified by the finer microstructure.

The third factor is related to the Nb segregation percentage that forms during the deposition. Indeed, lower laser power produced samples with higher Nb segregation and Laves phase as showed in Fig. 15. This contributes to the greater hardness and lower tensile strength which is compatible with the results obtained by Chen et al. [23]. Although, Nb segregation is considered as mainly responsible for the detrimental Laves phase formation that drastically affects the mechanical properties, however, the fine Laves phase formation does show characteristics which can increase the hardness of samples produced by lower laser power.

3.7. The effect of laser power on density and porosity

Porosity is formed by the gas that is dissolved in a liquid alloy and it starts to form pores. Usually, pores are created when the pressure within the pores exceeds the pressure within the interdendritic liquid, that a decrease of laser power leads to a decrease of the solubility of the gas elements [24]. It was also observed that high laser power leads to the production of samples that show higher laser density and reduced porosity than ones produced by lower laser power. This is compatible with the findings of Zhong et al. [11]. This trend was experimentally observed in the samples produced and the main results are reported in Fig. 18. Also, Kobryn et al. [25] showed

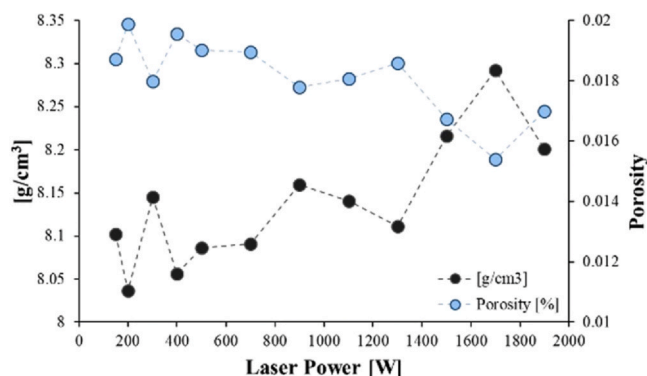


Fig. 18. Laser power effect on the density and the porosity.

that porosity can be reduced by increasing laser power and scanning speed. Overall, the porosity variations are rather limited due to the high quality of the powder, as evident through the lack of entrapped pores within the powder particles.

3.8. The effect of laser power on texture and phases (XRD)

The X-Ray diffraction patterns measured on walls produced by different levels of laser power are reported in Fig. 19. The section which was analysed on each sample is referred to as the x-z plane. The results of the powder analysis showed major peaks in the correspondence of (111), (200), (022), (311) and (222) with no other minor peaks. At low (400 W) and high (1500 W) laser power, the dominant peak switched from (111) to (200), which is also the preferred orientation of the material during DLD. However, when a laser power of 900 W was used, the intensity of the main peaks was comparable with those observed on the powder. The higher powers, e.g. 900 W and 1500 W, showed the formation of small peaks and this is because of decreased lattice parameters through depletion of the matrix of Nb and Laves phase formation. Precipitate phases such as γ'' (Ni_3Nb , BCT) and γ' ($\text{Ni}_3(\text{Al}, \text{Ti})$, FCC) have limited volume fraction, their peaks partially overlap with γ -Ni peaks and indirectly infer with the presence of intermetallic phases. These peaks appear because of thermal stress build-up which leads to Nb-segregation or precipitates formation in the microstructure. Carbides of M6C or MC types form at high temperatures, which explains the increase in peak intensity at 75° with the increase in laser power. Because of the high laser power and the accumulation of the heat input, which causes the build to be exposed to high temperatures for longer time, this leads to the formation of NbC which forms at $\sim 1250^\circ\text{C}$ during solidification. δ phase has been observed emanating from the NbC particles. Generally, MC and δ phase are detrimental for the mechanical properties. The presence of these phases at the grain

boundaries could improve the creep property if controlled as Sjöberg et al. [27].

3.9. Microstructural control using laser power

To demonstrate the effect of laser power variation in controlling and tailoring the microstructure, two thin walls were built varying the power in real time after a specified number of deposited layers. In detail, the deposition process consisted of two different laser powers. The first was set to 700 W for 20 layers and the second, a reduction to 200 W was performed. The microstructural analysis on the thin wall cross-section (y-z plane) showed that the grains columnarity was reduced from $760\ \mu\text{m}$ to $242\ \mu\text{m}$. After the heat accumulated, the grains became coarser and the grain ratio also increased. Higher power tends to produce wider spot sizes, and thus justifies the increase of the wall width when 700 W was used. The EBSD mapping was also performed on a cross-section of the samples (y-z plane perpendicular to the build direction) and x-z plane. In Fig. 20, the EBSD results are reported and suggest a drastic variation of the grain size as well as their morphology.

It is important to highlight that the grains observed in the region where lower laser power (200 W) was used are three times greater than those measured in the single walls (Fig. 10). The reason for this difference is mainly due to the different heat accumulation evolution. The first 20 layers were produced using higher laser power (700 W) which led to a higher accumulation of heat. However, the grains closer to the final region of the wall were smaller and a higher hardness was measured as expected. Moreover, the grain columnarity and width at the top region of the wall were reduced by 33% and 29% respectively. Finally, as shown in Fig. 20, the hardness measured on the y-z and x-z plane showed higher value compared with the bottom part and the increment measured in the x-z and the y-z plane is comparable at 23% and 20% respectively. The hardness on its own is insufficient to understand the mechanical performance at high temperatures, which will be explored in a future publication.

4. Conclusion

In this research, the microstructural characterization and the hardness of the IN718 single walls, fabricated using DLD, varying the laser power were investigated. Finally, the following results can be summarised:

- The microstructure and, in particular, the grains can be tailored to an average size by changing the heat input through different laser power values using a constant scan speed.
- An increase of the heat input increases the dendrite arm spacing (DAS) which indicates a decrease of the cooling rate. This is usually due to a decrease of the thermal gradient or a decrease of the velocity of the solidification front.

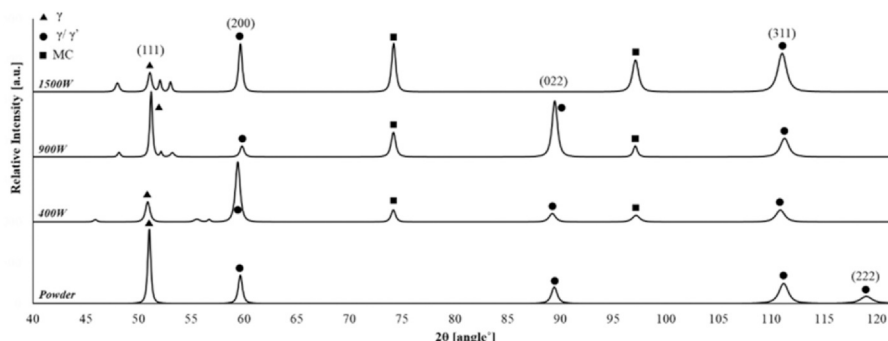


Fig. 19. X-ray diffraction patterns comparison of the samples produced by different laser powers.

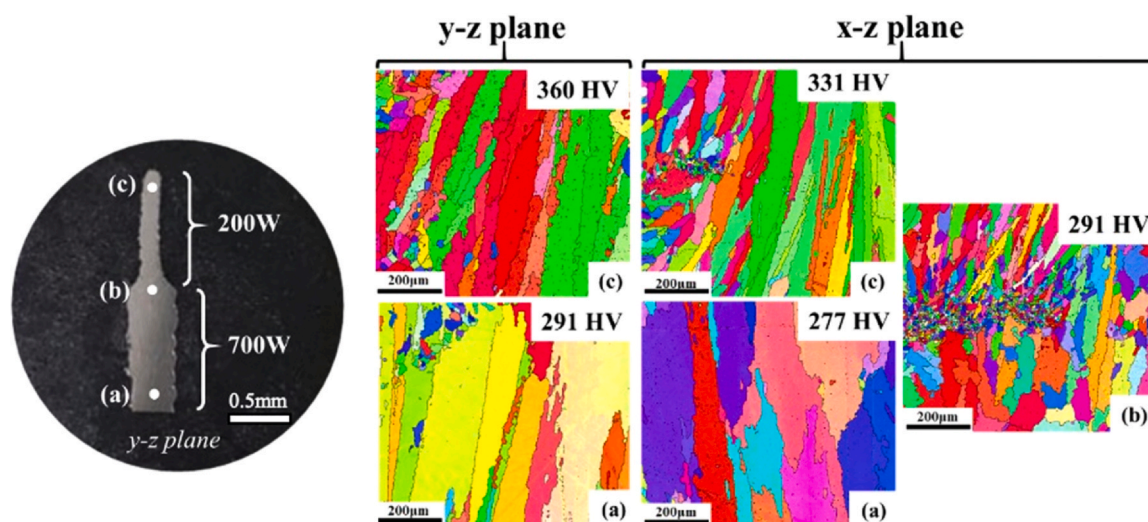


Fig. 20. Grain controlled sample.

- Electron microscopy confirmed the transition between equiaxed to columnar dendritic microstructure when the low laser power was increased to high, although no well-defined texture was developed.
- The hardness measured on the samples produced by low laser power showed slightly increased hardness than the samples produced by higher laser power. This is related to the microstructural size as smaller dendrite arms spacing increases hardness.
- Higher laser power led to a decrease of porosity and an increase of the density of the parts produced.
- An increase of laser power led to the formation of carbides due to higher heat accumulation during the DLD process. Their presence was confirmed by the X-Ray diffraction analysis.
- The Nb-segregation behaves differently depending on the location of the build, the cooling rate and the outside influences such as substrate and atmosphere.
- Nb-segregation decreases with an increase of heat input since the lower cooling rate allows the Nb to dissolve in the γ and γ' phases.

CRediT authorship contribution statement

Abdullah Alhuzaim: Designed the study and performed the experimental work and the analysis of the results as a part of his Ph.D. Wrote, reviewed and edited the manuscript. **Stano Imbrogno:** Contributed to the direct laser deposition experiments and thermal imaging, as well as the analysis of the results. Reviewing the paper. **Moataz M. Attallah:** Conceptualisation, supervision, support on experimental feasibility and infrastructure, writing – review and editing.

Declaration of Competing Interest

The authors declare that they have no known competing financial interests or personal relationships that could have appeared to influence the work reported in this paper.

Acknowledgments

Abdullah Alhuzaim would like to acknowledge the Royal Commission for Jubail and Yanbu, Kingdom of Saudi Arabia and the EU 4D Hybrid for the financial support.

Appendix A. Supplementary material

Supplementary data associated with this article can be found in the online version at doi:10.1016/j.jallcom.2021.159588.

References

- [1] D.D. Erick Schlienger, Michelle Griffith, Joseph Michael, Mike Oliver, Tony Romero, John Smugeresky, Near Net Shape Production of Metal Components Using LENS, 1998.
- [2] H. Xiao, S.M. Li, W.J. Xiao, Y.Q. Lia, L.M. Chab, J. Mazumder, L.J. Song, Effects of laser modes on Nb segregation and Laves phase formation during laser additive manufacturing of nickel-based superalloy, *Mater. Lett.* 188 (2017) 260–262.
- [3] H.B. Dong, P.D. Lee, Simulation of the columnar-to-equiaxed transition in directionally solidified Al-Cu alloys, *Acta Mater.* 53 (2005) 659–668.
- [4] M. Donachie, S.J. Donachie, *Superalloys A Technical Guide*, ASM International, 2002.
- [5] C.H. Radhakrishna, K. Prasad Rao, The formation and control of Laves phase in superalloy 718 welds, *Mater. Sci.* 32 (1997) 1977–1984.
- [6] Zhuqing Wang, T.A. Palmer, Allison M. Beese, Effect of processing parameters on microstructure and tensile properties of austenitic stainless steel 304L made by directed energy deposition additive manufacturing, *Acta Mater.* 110 (2016) 226–235.
- [7] Yuan Chen, K. Zhang, Jian Huang, Seyed Reza Elmi Hosseini, Zhuguo Li, Characterization of heat affected zone liquation cracking in laser additive manufacturing of Inconel 718, *Mater. Des.* 90 (2016) 586–594.
- [8] Lakshmi L. Parimi, Ravi G.A., Daniel Clark, Moataz M. Attallah, Microstructural and texture development in direct laser fabricated IN718, *Mater. Charact.* 89 (2014) 102–111.
- [9] L. Zhu, Z.F. Xu, P. Liu, Y.F. Gu, Effect of processing parameters on microstructure of laser solid forming Inconel 718 superalloy, *Opt. Laser Technol.* 98 (2018) 409–415.
- [10] R.G. Ding, Z.W. Huang, H.Y. Li, I. Mitchell, G. Baxter, P. Bowen, Electron microscopy study of direct laser deposited IN718, *Mater. Charact.* 106 (2015) 324–337.
- [11] A.G. Chongliang Zhong, Thomas Schopphoven, Reinhart Poprawe, Experimental study of porosity reduction in high deposition-rate laser material deposition, *Opt. Laser Technol.* 75 (2015) 87–92.
- [12] S. Tin, T.M. Pollock, Nickel-based superalloys for advanced turbine engines: chemistry, microstructure, and properties, *J. Propuls. Power* 22 (2006).
- [13] Narendran Raghavan, R. Dehoff, Sreekanth Pannala, Srdjan Simunovic, Michael Kirka, John Turner, Neil Carlson, Sudarsanam S. Babu, Numerical modeling of heat-transfer and the influence of process parameters on tailoring the grain morphology of IN718 in electron beam additive manufacturing, *Acta Mater.* 112 (2016) 303–314.
- [14] Abdullah Alhuzaim, R.B. Madigan, Measurement and simulation of low carbon steel alloy deposit temperature in plasma arc welding additive manufacturing, *Int. J. Innov. Educ. Res.* 2–06 (2014) 113–127.
- [15] David Gibson, R. Plume, Edwin Bergin, Sarah Ragan, Natalie Evans, Molecular line observations of infrared dark clouds. II. Physical conditions, *Astrophys. J.* 705 (2009) 123–134.
- [16] Lin Zhu, Z. Xu, Yuefeng Gu, Effect of laser power on the microstructure and mechanical properties of heat treated Inconel 718 superalloy by laser solid forming, *J. Alloy. Compd.* 746 (2018) 159–167.
- [17] H.L. Wei, T. Mukherjee, T. DebRoy, Grain growth modeling for additive manufacturing of nickel based superalloys, in: *Proceedings of the 6th International Conference on Recrystallization and Grain Growth*, 2016.

- [18] D.D. Gu, W. Meiners, K. Wissenbach, R. Poprawe, Laser additive manufacturing of metallic components: materials, processes and mechanisms, *Int. Mater. Rev.* 57 (2012) 133–164.
- [19] H.L. Wei, G.L. Knapp, T. Mukherjee, T. DebRoy, Three-dimensional grain growth during multi-layer printing of a nickel-based alloy Inconel 718, *Addit. Manuf.* 25 (2019) 448–459.
- [20] Ohmi Miyagawa, Masaru Yamamoto, Mitsuyuki Kobayashi, Zig-zag grain boundaries and strength of heat resisting alloys, *Superalloys (1976)* 245–254.
- [21] H. Qi, M. Azer, A. Ritter, Studies of standard heat treatment effects on microstructure and mechanical properties of laser net shape manufactured INCONEL 718, *Metall. Mater. Trans. A* 40 (2009) 2410–2422.
- [22] S. Azadian, Aspects of Precipitation in the Alloy Inconel 718, Department of Applied Physics and Mechanical Engineering, Division of Engineering Materials Luleå University of Technology, 2004.
- [23] Yuan Chen, Y. Guo, Mengjia Xu, Chunfei Ma, Qunli Zhang, Liang Wang, Jianhua Yao, Zhuguo Li, Study on the element segregation and Laves phase formation in the laser metal deposited IN718 superalloy by flat top laser and gaussian distribution laser, *Mater. Sci. Eng. A* 754 (2019) 339–347.
- [24] P.K. Sung, D.R. Poirier, S.D. Felicelli, E.J. Poirier, A. Ahmed, Simulations of microporosity in IN718 equiaxed investment castings, *J. Cryst. Growth* 226 (2001) 363–377.
- [25] P.A. Kobryn, E.H. Moore, S. Lee Semiatin, The effect of laser power and traverse speed on microstructure, porosity, and build height in laser-deposited Ti-6Al-4V, *Scr. Mater.* 43 (2000) 299–305.
- [26] L. Zhu, Z.F. Zhu, P. Liu, Y.F. Gu, Effect of processing parameters on microstructure of laser solid forming Inconel 718 superalloy, *Opt. Laser Technol.* 98 (2018) 409–415.
- [27] G. Sjöberg, N.-G. Ingesten, Grain Boundary S-Phase Morphologies, Carbides and Superalloys 718, 625 and Various Derivatives, 1991.